Published in: Chemical Physics (2000), vol. 256, pp. 239-249
Status : Postprint (Author's version)

Photoelectron spectroscopy of vinylbromide and intramolecular dynamics of the ionic $\tilde{B}$ state

A. Hoxha [a], R. Locht [a], B. Leyh [a,1], D. Dehareng [b], K. Hottmann [c], H. Baumgärtel [c]

[a] *Département de Chimie Générale et de Chimie Physique, Institut de Chimie Bât.B6c, Université de Liège, B-4000 Sart-Tilman (Liège 1), Belgium*
[b] *Centre d'Ingénierie des Protéines, Bât.B6c, Université de Liège, B-4000 Sart-Tilman (Liège 1), Belgium*
[c] *Institut für Physikalische und Theoretische Chemie, Freie Universität Berlin, Takustraße 3, D-14195 Berlin, Germany*
[1] *Chercheur qualifie du FNRS (Belgium).*

Abstract

In this paper, we report the He(I) photoelectron spectrum (PES) and the threshold-photoelectron (TPES) spectrum of C_2H_3Br. The fine structure observed in the first two ionic states in the He(I) spectrum is assigned to progressions belonging partially to previously unobserved vibrational normal modes. The TPES has been measured between 9.0 and 25.0 eV, and the photon energy range of 9.8-12.0 eV has been investigated in more detail. Extensive calculations with the GAUSSIAN set of programs have been performed to help in the assignment of the observed features. Furthermore, a conical intersection between the $\tilde{A}^2$ A" and the $\tilde{B}^2$A" states was found to take place along the C-Br stretching coordinate. Intramolecular dynamics of the $\tilde{B}^2$A" state, initially prepared in the Frank-Condon region, was probed by the Fourier transform of the spectrum. The $\tilde{B}^2$A" state is almost readily depleted, most probably due to a very effective internal conversion through the conical intersection.

1. Introduction

The halogenated derivatives of ethylene are useful model compounds to investigate the dynamics and energetics of medium-sized molecular ions and clusters. For this purpose, a good knowledge of the isolated molecule is a necessary starting point. In this framework, the spectroscopy of the fluorinated and chlorinated derivatives has been recently studied [1-3], and we present here the first results of a detailed study of bromo-ethylene.

The He(I)-photoelectron spectrum of C_2H_3Br at medium resolution has been investigated by several authors [4-6]. A low resolution threshold-photoelectron spectrum has been reported by Lohr et al. [7]. The vertical ionization energies have also been obtained by Green's function methods and confirmed by (e,2e) spectroscopy [8]. To our knowledge, no other theoretical work has been reported.

In this paper, we report an experimental study of the He(I)-photoelectron spectrum and the threshold-photoelectron spectrum at higher resolution compared with new computational results.

Section 2 briefly describes the experimental methods and the computational tools used. Section 3 focuses on the experimental and computational results, which will be discussed in Section 4. Forthcoming papers will deal with the photoab-sorption spectrum, constant ionic state spectroscopy as well as with the photoionization mass spectrometry of C_2H_3Br. The photodissociation dynamics of the $C_2H_3Br^+$ ion analyzed by the maximum entropy method has been presented in a previous paper [9].

2. Experimental and theoretical methods

2.1. Experimental

Two distinct experimental setups have been used for this work. The He(I) spectra have been obtained with a helium discharge lamp, giving a resonance line at 21.21 eV. The details of this spectrometer, designed for photoion-photoelectron coincidence spectroscopy, have been given elsewhere [10]. This is based on a Lindau-type electron energy analyzer. The raw spectra are corrected for the non-ideal transmission function of the analyzer and for the background signal. The energy scales of the spectra have been calibrated with respect to the

known ionization energies of inert gases (Ar/Kr/Xe mixture). In our best spectra, the accuracy on the position of the narrow peaks is estimated to be about 4 meV. To take into account experimental broadening factors, the spectra have been deconvoluted by a modified iterative algorithm [11,12] using a rare gas peak profile as apparatus function.

Threshold spectra were obtained using the vacuum UV light from the synchrotron radiation provided by the electron storage ring BESSY (Berlin). Details of this experimental setup and, more specifically, the electron energy analyzer used in these experiments have been outlined earlier [13] and will be discussed in a forthcoming paper. The light dispersed by a 3 m normal incidence mono-chromator (3m-NIM-l line) is focused into an ion chamber in the focusing plane of a tandem electron spectrometer consisting of two 180° electrostatic deflectors. The photon energy scale of the monochromator is calibrated with rare gas (Ar or Xe) threshold-photoelectron spectra. In the experiments reported in this paper, a full width at half maximum (FWHM) of less than 10 meV has been achieved. The photoelectron signal of a gold diode as well as the synchrotron storage ring beam current are measured in order to normalize the photoelectron signals in the TPES spectra. The TPES spectra are recorded by tuning the photon energy and transmitting only photoelectrons of a zero kinetic energy through the tandem electron energy analyzer system. Autoionization processes are known to play a significant role in such spectra [14]. Vinyl bromide (98% purity, inhibited with 200 ppm monoethyl hydroquinone) was commercially available (Aldrich Chem. Inc.) and was used without further purification.

2.2. Computational tools

All the calculations were performed with the GAUSSIAN 94 [15] set of programs, on two computers, a DEC 8400 with eight processors, and a DEC 4100 with four processors. All the investigated electronic state geometries were fully optimized. The calculation levels used for these optimizations were the following: the restricted Hartree-Fock (RHF) level [16-19] and the multi-configurational self-consistent field (SCF) level called complete active space SCF (CASSCF) [20-22] for the ground state of the neutral, the unrestricted Hartree-Fock (UHF) level [23] for the $\tilde{X}^2A''$ and $\tilde{A}^2A'$ states of the cation, the CASSCF and the configuration interaction expansion on all the single substitutions (CIS) [24] for the $\tilde{B}^2A''$ state of the cation. The basis set used was 6-311G [25-27] with diffuse (+) [28] and polarization (*) [29] functions on the heavy nuclei, labeled 6-311+G*. Two sets of (active electrons, active molecular orbitals) pairs were considered for both the neutral and the $\tilde{B}^2A''$ state of the cation: (4,4) and (8,7) for the neutral and (3,4) and (7,7) for the cation. In the following, the CASSCF calculations are denoted as CAS(n_e,n_{MO}), where n_e and n_{MO} are, respectively, the active electrons and active molecular orbitals numbers. The frequencies were determined analytically for all the optimized minima. No correcting factor was applied to these frequencies.

3. Results

3.1. Experimental results

3.1.1. The He(I)-photoelectron spectra

The He(I)-photoelectron spectrum of C_2H_3Br has been recorded over the whole ionization energy range available at medium resolution. At least seven well-defined bands can be observed in the complete deconvoluted PES spectrum shown in Fig. la. The observed vertical ionization energies are displayed in Table 1. The present measurements agree with those reported earlier [4-6, 8].

Except for the first two bands exhibiting sharp and intense peaks, the five remaining bands look more diffuse and continuous. However, a closer examination reveals a fine structure in the third band. The first three electronic bands have been investigated in more detail and are displayed in Fig. 2a-c.

3.1.2. The threshold-photo electron spectra

The threshold-photoelectron spectrum of C_2H_3Br has been investigated in the 9.0-25.0 eV photon energy range (Fig. lb). Compared to the He(I) spectrum, the 10.91 and 12.27 eV bands are superimposed on a broad unstructured continuum, while several weak and sharp features are present in the 10.2-11.6 eV region. As an example, and for a better visualization of these differences, the energy range 9.8-10.8 eV in both spectra is displayed in Fig. 3. For discussion purposes, a part of the photoabsorption spectrum, analyzed in a forthcoming paper, is also displayed in this figure. Another significant difference consists in the ionization cross-sections of

the successive ionic states. As previously observed in the cases of vinylchloride [1] and 1,1 difluoroethylene [3], several bands exhibit large differences of their relative intensity with respect to that observed in the He(I) spectrum.

Fig. 1: *(a) Deconvoluted He(I)-photoelectron spectrum of C_2H_3Br recorded between 9.0 and 20.0 eV and (b) threshold-photoelectron spectrum of C_2H_3Br recorded between 9.0 and 25.0 eV photon energy.*

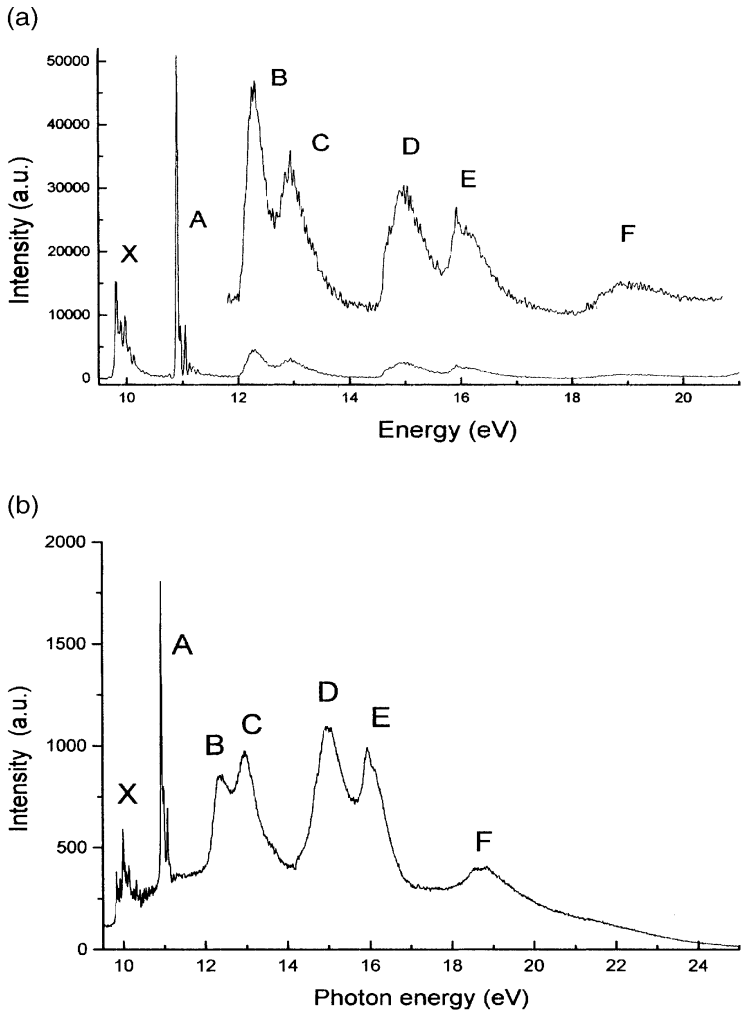

Table 1: *Vertical ionization energies of C_2H_3Br (in eV)*

State	He(I)				(e,2e), Ref. [8]	TPES, this work
	Ref. [4]	Ref. [5]	Ref. [6]	This work		
2a" ($C{=}C_{\Pi}$)	9.80	9.83	9.87	9.804	9.9	9.804
7a' (Br l.p.$^{\perp}$)	10.90	10.93	10.87	10.899	10.9	10.902
1a" (Br l.p.$^{\parallel}$)	12.28	12.33	12.30	12.27	12.3	12.34
6a'	12.94	12.97	12.93	12.95	13.4	12.95
5a'	15.02	14.98	15.05	14.90	15.4	14.94
4a'	16.21	15.94	16.07	15.93	16.5	15.91
3a'	19.20	18.55	18.75	18.87	19.0	18.7

l.p.$^{\perp}$ = lone pair of a" symmetry, l.p.$^{\parallel}$ = lone pair of a' symmetry.

Published in: Chemical Physics (2000), vol. 256, pp. 239-249
Status : Postprint (Author's version)

Fig. 2: *Expanded energy scale for the He(I)-photoelectron spectrum of (a) the $\tilde{X}^2A''$ state, (b) the $\tilde{A}^2A'$ state and (c) the $\tilde{B}^2A''$ state of $C_2H_3Br^+$. The vibrational analysis is included (see text).*

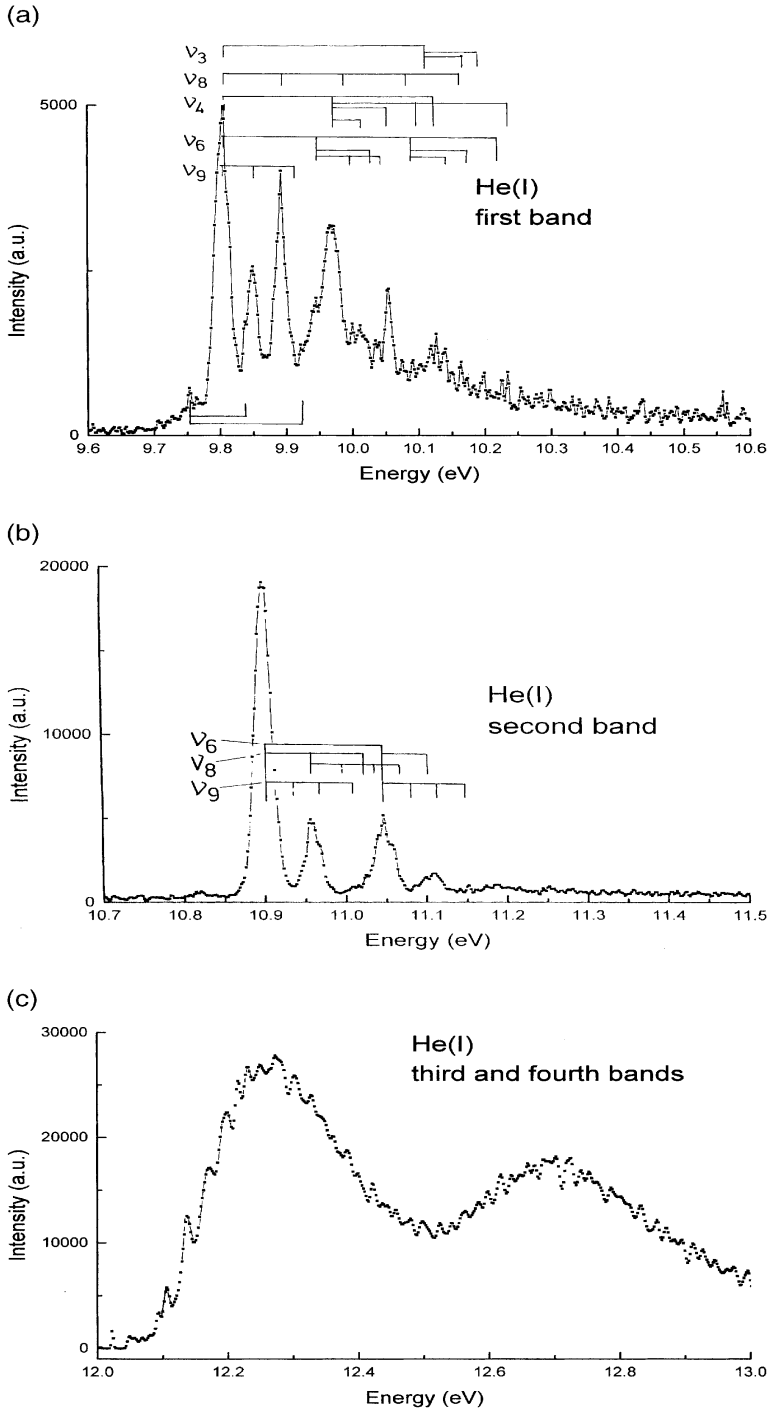

3.2. Computational results

In order to support the interpretation of the observed progressions and the normal mode assignments, ab initio calculations have been performed for the ground and excited states of the $C_2H_3Br^+$ ion. As a reference, the geometry and vibrational frequencies of the neutral molecule were also calculated; the results summarized in

Tables 2-4 are in good agreement with experimental data and previous calculations reported by Abrash et al. [30].

Fig. 3: *Threshold-photoelectron spectrum, He(I)-photoelectron spectrum and photoabsorption spectrum of C_2H_3Br recorded between 9.6 and 10.8 eV photon energy.*

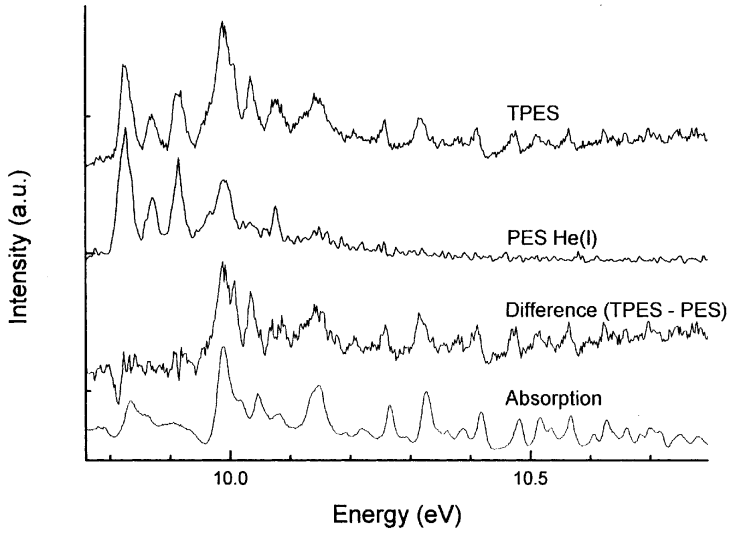

Fig. 4 shows a schematic representation of the nine optically active (a′ symmetry) normal modes of the X state of the ion. Calculated vibrational wave numbers of the neutral and ionic ground state and ionic excited states of $C_2H_3Br^+$ together with optimized geometries are reported in Tables 2 and 3. They provide a strong basis for the assignment of the observed progressions

Table 2: *Vibrational wave numbers (in cm^{-1}) of the ground state neutral molecule and of different ionic states of C_2H_3Br+*

Mode[a]	Neutral		$\tilde{X}\,^2A''$ ionic state		$\tilde{A}\,^2A''$ ionic state		$\tilde{B}^2A''$ ionic state
	Calculated[b]	Experiment[c]	Calculated[b]	Experiment[d]	Calculated*	Experiment[4]	Calculated"
ν_9 (a')	374.0	344	369.9	380	314.7	280	312.7
ν_8 (a')	649.9	613	747.1	710	443.7	460	1064.8
ν_{12} (a")	650.6	583	416.4		632.4		550.3
ν_{11} (a")	1067.9	902	923.5		959.1		554.6
ν_{10} (a")	1076.2	942	1086.7		1038.9		1122.1
ν_7 (a')	1116.1	1006	1141.8		1125.9		1361.8
ν_6 (a')	1400.0	1256	1368.7	1145	1324.7	1180	1578.9
ν_5 (a')	1525.0	1373	1505.7		1506.4		2072.0
ν_4 (a')	1801.5	1604	1642.3	1315	1767.7		2801.0
ν_3 (a')	3309.2	3027	3317.9	2540	3314.3		3314.7
ν_2 (a')	3390.7	3086	3381.6		3411.1		3403.5
ν_1 (a')	3405.9	3113	3441.9		3417.8		3419.7

[a] Normal modes are numbered according to the decreasing order of their wave numbers for each irreducible representation in the neutral molecule.
[b] H-F/6.311+G* level.
[c] From Ref. [30].
[d] Experimental accuracy is ±30 cm^{-1}.
[e] CIS/6-311+G* level.

In the framework of the Frank-Condon approximation, the ionization process is vertical, i.e. the vibrationless wave function of the neutral molecule is propelled on the potential energy surface of the ionic state.

Therefore, the gradient of the potential energy surface of the ion at the geometry of the neutral defines the force vector governing the initial motion of the wave packet. This gradient has been calculated at the CAS(7,7)/ 6-311+G* level for each ionic state at the geometry of the neutral molecule. This latter geometry has been optimized at the CAS(8,7)/6-311+G* level. The most important results are listed in Table 4.

Table 3: *Calculated geometric parameters for C_2H_3Br (distances are given in Å and angles in deg)*

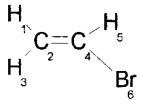

Internal coordinate	Neutral RHF/6-311+G*	$\tilde{X}\,^2$A" ionic state UHF/6-311+G*	$\tilde{A}^2$A' ionic state UHF/ 6-311+G*	$\tilde{B}\,^2$A" ionic state CIS/6-311+G*
C2-C4 bond length	1.3117	1.3936	1.3021	1.3474
C4-Br bond length	1.8953	1.7904	1.9934	2.1081
H1-C2 bond length	1.0759	1.0755	1.0769	1.0783
H3-C2 bond length	1.0740	1.0748	1.0738	1.0758
H5-C4 bond length	1.0714	1.0754	1.0715	1.0731
H3-C2-H1 angle	117.71	119.03	117.66	118.51
H1-C2-C4 angle	119.53	119.51	116.88	118.50
H5-C4-C2 angle	124.03	120.91	133.34	129.12
Br-C4-H5 angle	112.68	116.48	107.32	110.09

Table 4: *Largest gradient components calculated at the geometry of the neutral (hartree/bohr or hartree/rad)*

	C-C	C-Br	C-C(Br)-H5	H-C(H)-C
$\tilde{X}\,^2$A" ionic state	+0.0535	-0.0388	+0.1009	-0.0012
$\tilde{A}^2$A' ionic state	-0.0043	+0.0109	+0.0201	-0.0120
$\tilde{B}\,^2$A" ionic state	+0.0505	0.0462	-0.0039	-0.0043

Fig. 4*: Schematic representation of the optically active normal modes of the X state of the $C_2H_3Br^+$ ion calculated at the UHF/6-311+G* level.*

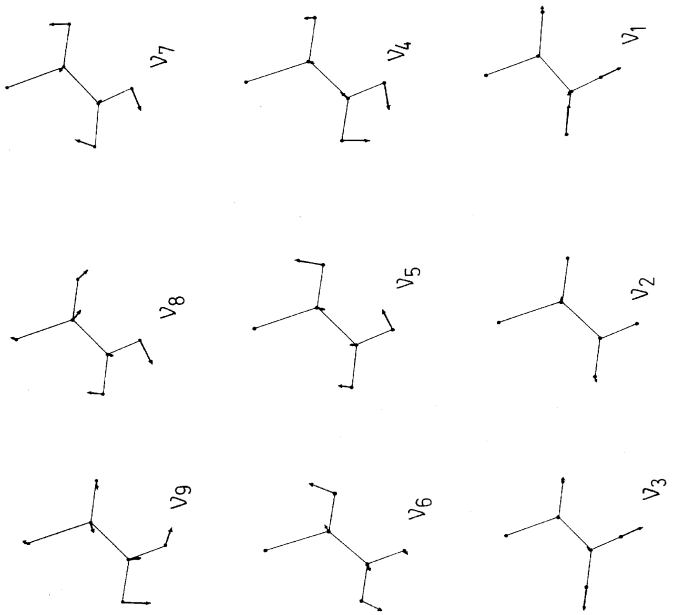

Published in: Chemical Physics (2000), vol. 256, pp. 239-249
Status : Postprint (Author's version)

4. Discussion

4.1. The He(I)-photoelectron spectrum of C_2H_3Br

In terms of a molecular orbital description, restricted to the valence and inner-valence orbitals, the electronic structure of the C_2H_3Br molecule in its ground electronic state (C_s symmetry) can be represented by

$$(1a')^2\ (2a')^2\ (3a')^2\ (4a')^2\ (5a')^2\ (6a')^2\ (1a'')^2\ (7a')^2 \times (2a'')^2\ \tilde{X}\,^1A'$$

Computation of the energies of the ionic states at the optimized geometry of the neutral leads to vertical ionization energies of 9.11, 10.04 and 11.64 eV for the first three ionic states. These values, calculated as E_{ion}[CAS(7,7)/6-311+G*]-$E_{neutral}$ [CAS(8,7)/6-311+G*], are in qualitative agreement with the experimental values listed in Table 1. The observed differences are most probably due to major changes in correlation energy between the neutral and the ion. However, if the energies of the exited ionic states are referenced with respect to the ground state of the ion, the computed values of 0.93 and 2.53 eV are in much better agreement with the corresponding experimental data (1.095 and 2.47 eV).

The ground state of the ion corresponds to the removal of the outermost electron of the neutral. According to the UHF calculations, the spin density is mainly located on the $C(H_2)$ atom (0.72), with relatively important components on the C(Br) (0.14) and Br (0.24) atoms. This supports the image of a delocalized π (a") orbital.

Fig. 2a shows the first ionic band. In agreement with previous results [4-6], three ionic vibrational modes can be easily deduced from the observed structure (Table 5). The first progression corresponds to ν_9 (CH_2 rocking) with a value of $\tilde{\nu}_9$ = 380 ± 30 cm^{-1}. The second one corresponds to the $\tilde{\nu}_8$ = 710 ± 30 cm^{-1} (C-Br stretching) while the third vibrational wave number of 1315 ± 30 cm^{-1} has been assigned to the ν_4 mode (CH_2 scissoring and C=C stretching). These three vibrational modes were observed in previous investigations [4-6]. Additional features observed in the present work are now discussed.

The peak measured at 9.946 eV can either be interpreted as the first member of another progression (ν_6 C=C stretching and H-C-C-H bending) or as the third member of the ν_9 progression. However, the existence of $\nu_6 + \nu_8$, as well as the absence of the lower combinations such as $\nu_9 + \nu_8$ and $2\nu_9 + \nu_8$ strongly favors the assignment to ν_6 with a wave number of 1145 ± 30 cm^{-1}.

Above 10.119 eV, a certain number of peaks listed in Table 5 do not fit into any of these four progressions. They could be interpreted as belonging to a previously unobserved vibrational mode $\tilde{\nu}_3$ = 2540 ± 30 cm^{-1} (C-H stretching) and its combinations.

The small peak observed at 400 cm^{-1} below the first IP is assigned to a hot band. It is supposed to arise from vibrationally excited neutral molecules, probably the ν_9 (344 ± 30 cm^{-1}) vibrational mode. Its intensity is 13% of the 0-0 transition while a Maxwell-Boltzmann distribution would give 18%. The difference reflects a nonunitary Franck-Condon factor. The hypothesis of the hot band is also supported by the presence of small peaks belonging to progressions starting from this hot band. The complete analysis of the vibrational structure, including the proposed assignments, is given in Table 5.

Referring to Table 2 and Fig. 4, the most important observed vibrational modes $\tilde{\nu}_9$ = 380 ± 30 cm^{-1}, $\tilde{\nu}_8$ = 710 ± 30 cm^{-1}, $\tilde{\nu}_4$=1315 ± 30 cm^{-1} correspond to the CH_2 rocking, C-Br stretch and (C=C stretch + CH_2 scissoring), respectively. In keeping with the calculations, the $\tilde{\nu}_6$ = 1315 ± 30 cm^{-1} mode can tentatively be assigned to the C=C stretching with both CH_2 and Br-C-H scissoring while the $\tilde{\nu}_3$ = 2540 ± 30 cm^{-1} could be ascribed as a CH_2 symmetric stretching.

The second photoelectronic band corresponds to the first ionic excited state. According to calculations at the UHF/6-311+G* level in the C_s symmetry, the ejected photoelectron pertains to the 7a' in-plane bromine lone pair, which is supposed to have a rather nonbonding character. Indeed, according to Table 3, small changes in geometry are induced by this ionization. They mainly involve the C-Br and C-C distances and the C-C-H angle (Table 3). The spin density is almost localized on the bromine atom. This is in agreement with the small extension of the vibrational structure. Two main vibrational wave numbers have been reported corresponding to

the excitation of the ν_8 and ν_6 vibrational modes. The wave numbers determined in this work, respectively, 460 ± 30 and 1180 ± 30 cm^{-1} are in good agreement with those reported previously in the literature [4-6]. A careful examination of the spectrum reveals the presence of a third vibrational progression assigned to the $\tilde{\nu}_9$ = 280 ± 30 cm^{-1} vibration. These assignments are in keeping with the above-mentioned geometrical modifications (see also Table 6).

Table 5: *Energy levels (eV), tentative assignments (0 means vibrationless level) and predicted energy of the fine structure observed in the He(I) and TPES spectra of $C_2H_3Br^+$ $\tilde{X}\,^2A''$ state*

He(I)	TPES	Assignment	Predicted
9.753		Hot band	
9.804	9.804	0	
9.839		h.b. + ν_8	9.841
9.850	9.852	ν_9	9.851
9.893	9.892	ν_8	9.892
9.902	9.900	$2\nu_9$	9.898
9.921		h.b. + ν_4	9.920
9.946	9.948	ν_6	9.946
9.968	9.970	ν_4	9.967
9.989		$2\nu_8$	9.980
9.999	9.996	$\nu_6 + \nu_9$	9.993
10.011	10.016	$\nu_4 + \nu_9$	10.014
10.035		$\nu_6 + \nu_8$	10.034
10.041	10.046	$\nu_6 + 2\nu_9$	10.040
10.053	10.054	$\nu_4 + \nu_8$	10.055
10.074	10.068	$3\nu_8$	10.068
10.092		$2\nu_6$	10.088
10.103		$\nu_4 + \nu_6$	10.109
10.119	10.122	ν_3	10.119
10.128	10.132	$2\nu_4$	10.130
10.140		$2\nu_6 + \nu_9$	10.140
10.152		$4\nu_8$	10.156
10.164		$\nu_3 + \nu_9$	10.166
10.174	10.188	$2\nu_6 + \nu_8$//	10.176//
		$2\nu_4 + \nu_9$	10.177
10.199		$\nu_3 + \nu_8$	10.207
10.226		$3\nu_6$	10.230
10.248	10.240	$\nu_4 + 2\nu_6$	10.251
	10.296	$3\nu_4$	10.293
	10.362	$4\nu_6$	10.372
	10.394	$3\nu_6 + 2\nu_8$	10.406
	10.458	$4\nu_4$	10.456
	10.492	$2\nu_4 + 2\nu_6 + \nu_8$	10.502
	10.546	$4\nu_4 + \nu_8$	10.544
	10.604	$4\nu_4 + \nu_6$	10.598
	10.640	$6\nu_6$	10.656
	10.680	$6\nu_6 + \nu_9$	10.700
	10.732	$6\nu_6 + \nu_8$	10.744

The third photoelectronic band, displayed in Fig. 2c, corresponds to the ionization of the la" electron (the bromine out-of-plane lone pair). A regular pattern characterized by a spacing of 250 ± 30 cm^{-1} is observed. This progression has been reported by Mines and Thompson [5] with a vibrational interval of 300 cm^{-1} and assigned to the excitation of the C-Br bending mode i.e. the ν_8 mode. However, as shown below, the situation is probably more complex, and an alternative interpretation will be proposed.

Attempts to optimize the $\tilde{B}$ state in the C_s symmetry at the UHF level failed. Yet, when optimized in

the C_1 symmetry at the CIS level, the B state adopts an almost planar geometry. It is interesting to note that, at its own equilibrium geometry, the $\tilde{B}\,^2A''$ state is lower in energy than the $\tilde{A}^2A''$ state. This reveals the existence of a potential energy surface crossing along a coordinate connecting the minima of the $\tilde{A}^2A'$ and $\tilde{B}\,^2A''$ states (mainly a C-Br stretching). Along a coordinate that lowers the symmetry group to C_1 (an out-of-plane motion), the two states involved belong to the same irreducible representation and hence repel each other. This is a typical conical intersection situation [31].

Table 6: *Energy levels (eV), tentative assignments (0 means vibrationless level) and predicted energy of the fine structure observed in the He(I) and TPES spectra of the C_2H_3Br+ $\tilde{A}^2A'$ state*

He(I)	TPES	Assignment	Predicted
10.899	10.902	0	
(10.934)		ν_9	10.934
10.956	10.961	ν_8	10.956
10.968		$2\nu_9$	10.969
11.007		$3\nu_9$	11.004
11.014	11.017	$2\nu_8$	11.013
11.024	11.023	$\nu_8 + 2\nu_9$	11.026
11.045	11.051	ν_6	11.045
11.058	11.065	$\nu_8 + 3\nu_9$	11.061
11.085	11.085	$\nu_6 + \nu_9$	11.080
11.100	11.103	$\nu_6 + \nu_8$	11.102
11.108		$\nu_6 + 2\nu_9$	11.115
11.151		$\nu_6 + 3\nu_9$	11.150
	11.219	$2\nu_6 + \nu_9$	11.226

According to Table 4, the predominant forces to which the system is initially submitted lie along the C=C and C-Br coordinates. In terms of normal modes of the $\tilde{B}\,^2A''$ state, the C-Br stretching has important components on the ν_8 (550 cm^{-1}) and ν_4 (2801 cm^{-1}) vibrations while the C=C stretching is involved in the ν_7 (1362 cm^{-1}) and ν_4 (2801 cm^{-1}) vibrations. From this analysis, it is clear that none of these expected normal modes would give rise to a wave number in the 250 cm^{-1} range. In the next section, we try to address the significance of the observed regular pattern and to get further insight into the intramolecular dynamics of the B state.

4.2. Intramolecular dynamics of the $\tilde{B}\,^2A''$ state

It is clear that the observed wave number, though not directly related to a normal mode, must reflect the periodicity of the motions of the vibrational wave packet on the potential energy surface of the $\tilde{B}\,^2A''$ state. Upon photoionization to the $\tilde{B}\,^2A''$ state, the system is prepared in the Franck-Condon region, and at the initial time ($t = 0$), it can be represented as a Gaussian wave packet corresponding to the vibrationless wave function of the neutral molecule. This wave packet is nonstationary on the potential energy surface of the $\tilde{B}\,^2A''$ state and propagates according to the main forces to which it is submitted. In our case, it moves along the C=C and C-Br coordinates (Table 4). According to the Ehrenfest theorem [32], the center of the wave packet representing the system undergoes the same motion as that of a classical particle. In the case of a harmonic oscillator, the center of the wave packet performs a regular motion. However, our situation is far from being harmonic. At the conical intersection, the wave packet is expected to split into two parts one of which remains on the initial ($\tilde{B}$ state) potential energy surface and can be reflected back, while the other part undergoes a nonadiabatic transition and evolves on the potential energy surface of the A state. The observed progression is then believed to be related to the periodicity of the motion of the part of the wave packet remaining in the $\tilde{B}$ state.

An interesting way to get information about the dynamics of evolution of a given electronic state in the femtosecond time range is to determine its autocorrelation function. The autocorrelation function, $C(t)$, gives the overlap of the initial ($\Phi(t = 0)$) and the propagated ($\Phi(t)$) wave packets. It is related to the spectral profile I(E) through a Fourier transform [33]:

$$C(t) = \langle \Phi(0) | \Phi(t) \rangle = \int_0^\infty I(E) \exp\left(\frac{-\mathrm{i}Et}{h}\right) \mathrm{d}E.$$

The correlation function of the $\tilde{B}$ state has been determined after removing the underlying contribution of the $\tilde{C}$ band and the constant background. As shown in Fig. 5, the calculation of *C(t)* shows a first meaningful recurrence time (≈1.7 x 10^{-13} s) where only a very small fraction of the wave packet (less than 3%) is reflected back to its initial location. Most probably, the largest majority of the system undergoes a rapid non-radiative transition to the $\tilde{A}$ state through the above-mentioned conical intersection. Conical intersections are indeed known to be very efficient funnels [34]. Consequently, the evolution of the system initially in the $\tilde{B}$ state can be characterized by two different life times. One of them is very short (10^{-13} s) and corresponds to the global width of the diffuse band in the photoelectron spectrum while part of the system has a longer lifetime and gives rise to the fine structure observed superimposed on the broad $\tilde{B}$ band.

4.3. Threshold-photoelectron spectrum

As mentioned earlier (Section 2), the first major discrepancy between the TPE and the He(I)-photoelectron spectra is the large difference of the relative intensities of the successive ionic bands. Taking the second band at 10.899 eV as reference, only the first ionic state shows roughly the same intensity in both spectra. All higher-lying photoelectron bands, observed between 12-20 eV photon energy exhibit much larger relative intensities in the TPE spectrum. The relative intensities are even reversed for the $\tilde{B}$ and $\tilde{C}$ bands. These observations would at least partially indicate a strong contribution of autoionization. This could be anticipated from the photoabsorption spectrum.

***Fig. 5**: Autocorrelation function C(t) corresponding to the spectral profile of the $\tilde{B}\,^2A''$ state of $C_2H_3Br^+$.*

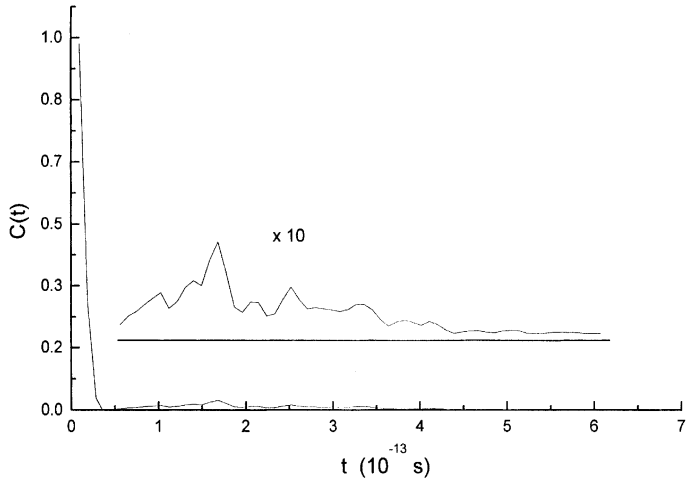

Furthermore, the photon energy region of 9.9-12 eV of the TPE spectrum shows additional features. In this range, a fairly intense continuum-like band is buried under the first two bands observed at 9.804 and 10.903 eV, respectively. However, a close examination of the second band shows no significant difference between the two spectra (Table 6).

The largest differences are observed for the $\tilde{X}$ band where the vibrational structure extends up to about 10.8 eV in the TPE spectrum, whereas the same band cuts off at 10.26 in the He(I)-photo-electron spectrum. The maximum intensity corresponds to the 0-1 ν_4 transition in the former and 0-0 transition in the latter. The position in energy of the additional structures are listed in Table 5. The absence of these features in the He(I) photoelectron allows us to ascribe them to the autoionization of Rydberg states belonging to series converging to the second ionization threshold of C_2H_3Br. Comparison with the photoabsorption spectrum strongly supports this interpretation. Fig. 3 clearly shows the correlation between the photoabsorption peaks assigned to members of Rydberg series and the features observed in the TPES spectrum. As previously mentioned, the photoabsorption will be dealt with in a separate paper.

The assignments proposed in the third column of Tables 5 and 6 are obtained as follows. The observed structures must correspond to vibrational levels of the $C_2H_3Br^+$ $\tilde{X}^2A''$ and $\tilde{A}^2A'$ ionic states. The fourth columns of Tables 5 and 6 report the calculated positions of the vibrational levels based on wave number values given in Table 2. The unknown anharmonicity has been neglected. The agreement between the experimental and predicted energies is very satisfactory (standard deviation = 7 meV for the $\tilde{X}^2A'$ state and even less for the $\tilde{A}^2A'$ state). This strongly supports the proposed assignments.

5. Concluding remarks

In this work, the electronic and vibrational spectroscopy of the valence states of ionized vinyl bromide has been studied by resonance line PES, TPES and ab initio calculations. Deconvolution allowed us to perform a detailed vibrational analysis of the first two ionic states. Previously unknown normal modes of the ground state and of the first excited state of the $C_2H_3Br^+$ ion are reported. They correspond to the ν_6 (C=C stretching with CH_2 and CHBr scissoring) and the ν_3 (CH_2 symmetric stretching) modes for the ground ionic state and to the ν_9 (CH_2 rocking) for the first excited ionic state. The assignments are based on ab initio calculations of geometry changes upon ionization and analytical calculation of wavenumbers at optimized minima.

These calculations suggested the existence of a conical intersection between the $\tilde{A}$ and the $\tilde{B}$ states of $C_2H_3Br^+$ along the C-Br coordinate. The frequency observed in the $\tilde{B}$ state, formerly assigned to a C-Br bending mode is believed to unveil, instead, the periodicity of the first motions of the wave packet representing the system. The autocorrelation function, obtained by Fourier transform of the $\tilde{B}$ state spectrum, shows that at the first recurrence time, only nearly 3% of the wave packet representing the system comes back to the Franck-Condon region. Most of the $\tilde{B}$ state population undergoes a nonadiabatic transition to the $\tilde{A}^2A'$ state.

Acknowledgements

We are grateful to Dr. A.J. Lorquet, who performed some preliminary ab initio calculations of the vibrational modes of C_2H_3Br and $C_2H_3Br^+$. The authors are indebted to the University of Liege and to the FRFC (Fonds de la Recherche Fondamentale Collective). This work has been supported by the "Actions de Recherche Concerted (ARC)" (Direction de la Recherche Scien-tifique - Communauté Française de Belgique). AH, RL and BL acknowledge the European Community for financing this work through its Human Capital and Mobility Programme (Contract no. ERBFMGE-CT 97-0123). BL is indebted to the FNRS (Belgium) for a research associate position. Financial support of the Fonds des Chemischen Industrie is gratefully acknowledged by HB**.**

References

[1] R. Locht, B. Leyh, K. Hottmann, H. Baumgärtel, Chem. Phys. 220 (1997) 217.

[2] R. Locht, B. Leyh, K. Hottmann, H. Baumgärtel, Chem. Phys. 220 (1997) 207.

[3] B. Leyh, R. Locht, K. Hottmann, H. Baumgärtel, submitted for publication.

[4] D. Chadwick, D.C. Frost, A. Katrib, C.A. McDowell, R.A.N. McLean, Can. J. Chem. 50 (1972) 2642.

[5] G.W. Mines, H. Thompson, Proc. Roy. Soc. Lond. A 315 (1970) 32.

[6] K. Wittel, H. Bock, Chem. Ber. 107 (1974) 307.

[7] W. Lohr, H.W. Jochims, H. Baumgärtel, Ber. Bunsenges. Phys. Chem. 79 (1975) 901.

[8] R. Cambi, G. Ciullo, A. Sgamellotti, F. Tarantelli, R. Fantoni, A. Giardini-Guidoni, I.E. McCarthy, V.D. Martino, Chem. Phys. Lett. 101 (1983) 477.

[9] A. Hoxha, R. Locht, A.J. Lorquet, J.C. Lorquet, B. Leyh, J. Chem. Phys. 111 (1999) 9259.

[10] R. Locht, C. Servais, Z. Phys. Chem. 195 (1996) 153.

[11] R. Locht, G. Caprace, J. Momigny, Chem. Phys. Lett. 111(1984) 560.

[12] K.A.G. Macneil, J.C.J. Thyne, Int. J. Mass Spectrom. Ion Phys. 3 (1969) 35.

[13] K. Hottmann, H.-W. Jochims, H. Baumgartel, BESSY Jahresbericht, 398 (1987).

[14] T. Baer, P.M. Guyon, J. Chem. Phys. 85 (1986) 4765.

[15] M.J. Frisch, G.W. Trucks, H.B. Schlegel, P.M.W. Gill, B.G. Johnson, M.A. Robb, J.R. Cheeseman, T.A. Keith, G.A. Petersson, J.A. Montgomery, K. Raghavachari, M.A. Al-Laham, V.G. Zakrzewski, J.V. Ortiz, J.B. Fores-man, J. Cioslowski, B.B. Stefanov, A. Nanayakkara, M. Challacombe, C.Y. Peng, P.Y. Ayala, W. Chen, M.W. Wong, J.L. Andres, E.S. Replogle, R. Gomperts, R.L. Martin, D.J. Fox, J.S. Binkley, D.J. Defrees, J. Baker, J.P. Stewart, M. Head-Gordon, C. Gonzalez, J.A. Pople, GAUSSIAN 94, Revision D.4 (1996), Gaussian, Pittsburg, PA.

[16] D.R. Hartree, Proc. Camb. Phil. Soc. Math. Phys. Sci. 24 (1928) 426.

[17] V.A. Fock, Z. Phys. 61 (1930) 126.

[18] C.C.J. Roothaan, Rev. Mod. Phys. 23 (1951) 69.

[19] G.G. Hall, Proc. Roy. Soc. 208 (1951) 328.

[20] D. Hegarty, M.A. Robb, Mol. Phys. 38 (1979) 1795.

[21] R.H.E. Eade, M.A. Robb, Chem. Phys. Lett. 83 (1981) 362.

[22] F. Bernardi, A. Bottini, J.J.W. McDougall, M.A. Robb, H.B. Schlegel, Faraday Symp. Chem. Soc. 19 (1984) 137.

[23] J.A. Pople, R.K. Nesbet, J. Chem. Phys. 22 (1954) 571.

[24] J.B. Foresman, M. Head-Gordon, J.A. Pople, M.J. Frisch, J. Phys. Chem. 96 (1992) 135.

[25] A.D. McLean, G.S. Chandler, J. Chem. Phys. 72 (1980) 5639.

[26] R. Krishnan, J.S. Binkley, R. Seeger, J.A. Pople, J. Chem. Phys. 72 (1980) 650.

[27] L.A. Curtiss, M.P. McGrath, J.-P. Blaudeau, N.E. Davis, R.C. Binning Jr., L. Radom, J. Chem. Phys. 103 (1995) 6104.

[28] T. Clark, J. Chandrasekhar, G.W. Spitznagel, P.v.R. Shleyer, J. Comp. Chem 4 (1983) 294.

[29] M.J. Frisch, J.A. Pople, J.S. Binkley, J. Chem. Phys. 80 (1984) 3265.

[30] S.A. Abrash, R.W. Zehner, G.J. Mains, L.M. Raff, J. Phys. Chem. 99 (1995) 2959.

[31] J.C. Lorquet, in: T. Baer, C.Y. Ng, I. Powis (Eds.), The Structure, Energetics and Dynamics of Organic Ions, Wiley, Chichester, 1996.

[32] C. Cohen-Tanoudji, B. Diu, F. Laloe, Quantum Mechanics, Hermann, Paris, 1977.

[33] A.J. Lorquet, J.C. Lorquet, J. Delwiche, M.J. Hubin-Franskin, J. Chem. Phys. 76 (1982) 4692.

[34] H Köppel, W. Domcke, L.S. Cederbaum, Adv. Chem. Phys. 57 (1984) 59.